www.elsevier.nl/locate/jorganchem

Journal of Organometallic Chemistry 622 (2001) 155–165

Journal of Organometallic Chemistry

Palladium(0)–olefin complexes with potentially terdentate nitrogen–sulfur ligands. The role of the chelate in the olefin exchange path

Luciano Canovese *, Fabiano Visentin, Gavino Chessa, Graziano Gardenal, Paolo Uguagliati

Dipartimento di Chimica, Universita' di Venezia, Calle Larga Santa Marta 2137-30123 Venezia, Italy

Received 22 September 2000; accepted 7 November 2000

Abstract

The synthesis and the reactivity of Pd(0) olefin complexes [Pd(η^2-olefin)(SNS)] and [Pd(η^2-olefin)(NSN)] containing potentially terdentate nitrogen–sulfur ligands were studied. The presence of a potentially coordinating atom in the environment of the metal, influences strongly the fluxional behavior in solution but not the overall reactivity with respect to olefin exchange and thermodynamic stability which is very close to that of the corresponding bidentate nitrogen–sulfur complexes. The intimate mechanism of olefin exchange also involves a path promoted by the third dangling coordinating atom which induces olefin dissociation and stabilizes the ensuing Pd(0) three-coordinated species.

Keywords: Pallidium(0)–olefin complexes; Terdentate nitrogen–sulfur ligands; Olefin exchange path

1. Introduction

Zero valent palladium complexes are assumed to be intermediates in a number of stoicheiometric and catalytic processes involving C–C or C–N bond formation, such as cross-coupling [1], Heck [2], allyl alkylation [3] and amination [4]. In spite of their great importance, there is a paucity of studies on these species. As a part of our systematic investigations on attacks on palladium–allyl complexes by a variety of nucleophiles, we often examined Pd(0) substrates containing different ancillary ligands and electron poor olefins [4a,b,5]. In this context, we determined the equilibrium constants of olefin exchange between various metal substrates and the rates of such exchange processes when the hindered olefin tetramethylethylenetetracarboxylate (tmetc) was involved [6]. Based on these and other investigations [7] we concluded that comparatively stable species, while lending themselves to structural and reactivity studies, are less useful as catalytic agents. In searching for a reasonable compromise between stability and reactivity, we devised to study palladium(0) complexes of electron-deficient olefins and potentially terdentate S–N–S or N–S–N pyridin-thioether ligands. Indeed, these chelating agents are known to behave as bidentate ligands imparting a degree of stability similar to that of analogous complexes with related, truly bidentate chelating moieties [5g], while the dangling uncoordinated arm induces a general fluxionality in solution, liable to promote dissociation of the olefin fragment and stabilization of the ensuing three-coordinated palladium(0) species. Similar goals were sought by other authors using different P–N–N hemilabile ligands [8]. To the best of our knowledge, no sulphur–nitrogen donor ligands have been studied so far to this purpose. The complexes investigated and the olefins employed are shown in Scheme 1 and Table 1.

* Corresponding author. Tel.: +39-41-5298567/5298568; fax: +39-41-5298517.

E-mail address: Cano@unive.it (L. Canovese).

0022-328X/01/$ - see front matter
PII: S0022-328X(00)00870-6

[Pd(η^2-ol)(LL'L)]

LL'L = SNS(R) =

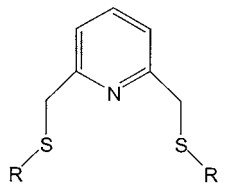

R = Me , Et , *i*-Pr , *t*-Bu , Ph

ol = ma , nq , tmetc , fn

LL'L = NSN =

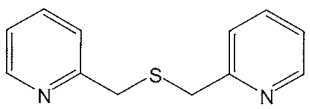

ol = ma , nq , tmetc

ma= maleic anhydride ; nq = naphthoquinone ;
tmetc = tetramethylethylenetetracarboxylate ;
fn = fumaronitrile

Scheme 1.

2. Results and discussion

2.1. Olefin exchange rates

The rates of olefin exchange in Pd(0) systems are in general comparatively high and correspond to associative mechanisms. Thus, the reactions are sensitive to steric hindrance, so that use of a sterically demanding olefin such as tmetc will slow down the process to rate values measured easily by customary spectrophotometric techniques. We have already exploited these features to gain intimate mechanistic information on related bidentate complexes [6]. We have now extended this study to complexes containing the present potentially terdentate ligands (see Scheme 1).

The complexes [Pd(η^2-nq)(SNS(R))] (R = Me, Et, *i*-Pr, *t*-Bu, Ph) and [Pd(η^2-nq)(NSN)] containing the chromophoric olefin 1,4-naphthoquinone were reacted with tmetc in $CHCl_3$. The course of the reaction was followed by UV–Vis spectrophotometric techniques in the range 600–330 nm in the presence of a constant excess of tmetc over the metal substrate ($[Pd]_0 = 1 \times 10^{-4}$ mol dm^{-3}) in order to ensure pseudo-first order conditions and to minimize the contribution of the reverse reaction to the overall spectral changes. Under these conditions the absorbance D_t obeys the mono-exponential rate law $D_t = D_\infty + (D_o - D_\infty)\exp(-k_{obs}t)$ where D_o, D_∞ and k_{obs} are the initial, final absorbances and the observed rate constants, respectively. The k_{obs} values, determined by non-linear regression where D_o, D_∞ and k_{obs} are the parameters to be optimized, fit the expression

$$k_{obs} = k_1 + k_2[\text{tmetc}] \quad (1)$$

in the case of complexes [Pd(η^2-nq)(SNS(R))] (R = *i*-Pr, *t*-Bu,Ph) (Fig. 1).

In the case of [Pd(η^2-nq)(SNS(Et))] and [Pd(η^2-nq)(NSN)] the expression which would fit better the k_{obs} values is:

$$k_{obs} = k_2[\text{tmetc}] \quad (2)$$

the intercept being statistically insignificant. With the complex [Pd(η^2-nq)(SNS(Me))] a general decomposition taking place in the reacting mixture prevents any measurements.

A suitable mechanism for fitting these results is shown in Scheme 2, which also involves rate determining first-order formation of an olefin-free Pd(0) intermediate **I** which subsequently reacts rapidly with tmetc to yield the final olefin exchange product [Pd(η^2-tmetc)(SNS(R))]. Under the kinetic conditions pertaining to data in Table 2, Scheme 2 reduces to Scheme 3 and will yield rate law Eq. (1). As for the nature of intermediate **I**, we have no evidence to rule out the presence of a solvent molecule in the coordination sphere of the metal along with the terdentate ligand SNS(R), even though a coordinatively unsaturated, solvent-free three-coordinated species is not without precedent [8].

The occurrence of a first-order path k_1, when observable (Table 2), can be traced back to the capability of the dangling arm bearing a coordinating atom in the potentially terdentate ligands SNS(R) to stabilize an

Table 1
Complexes under study

[Pd(η^2-ma)(SNS(Me))]	[Pd(η^2-nq)(SNS(Me))]		[Pd(η^2-fn)(SNS(Me))]
[Pd(η^2-ma)(SNS(Et))]	[Pd(η^2-nq)(SNS(Et))]	[Pd(η^2-tmetc)(SNS(Et))]	[Pd(η^2-fn)(SNS(Et))]
[Pd(η^2-ma)(SNS(*i*-Pr))]	[Pd(η^2-nq)(SNS(*i*-Pr))]	[Pd(η^2-tmetc)(SNS(*i*-Pr))]	
[Pd(η^2-ma)(SNS(*t*-Bu))]	[Pd(η^2-nq)(SNS(*t*-Bu))]	[Pd(η^2-tmetc)(SNS(*t*-Bu))]	[Pd(η^2-fn)(SNS(*t*-Bu))] [a]
[Pd(η^2-ma)(SNS(Ph))]	[Pd(η^2-nq)(SNS(Ph))]	[Pd(η^2-tmetc)(SNS(Ph))]	
[Pd(η^2-ma)(NSN)]	[Pd(η^2-nq)(NSN)]	[Pd(η^2-tmetc)(NSN)]	[Pd(η^2-fn)(NSN)]

[a] Complex obtained from amination reaction of the corresponding allyl species (see text).

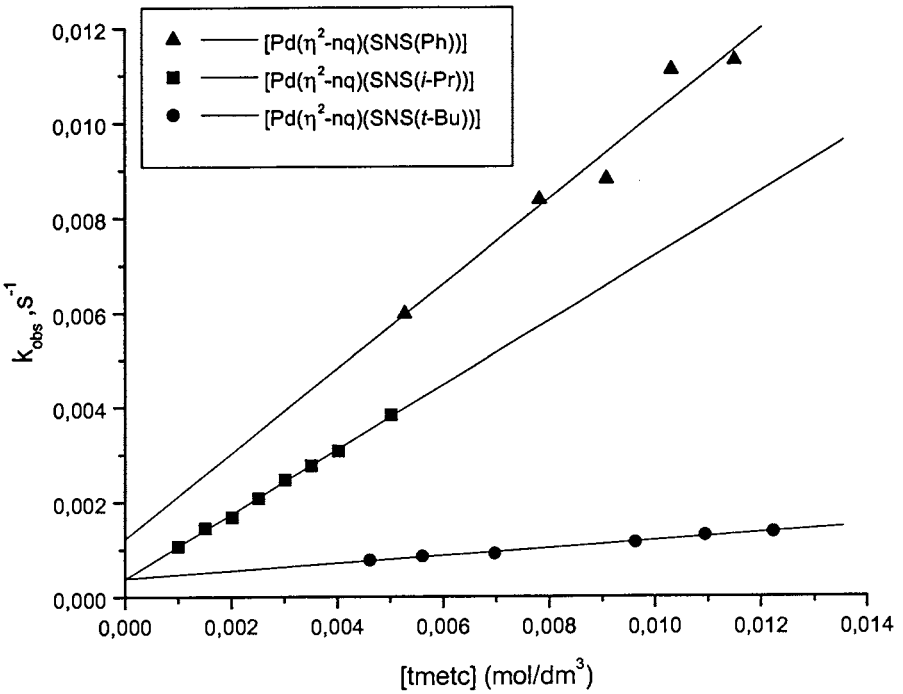

Fig. 1. Fit of k_{obs} values to added tmetc concentration for the reaction $[Pd(\eta^2\text{-nq})(SNS(R))] + tmetc = [Pd(\eta^2\text{-tmetc})(SNS(R))] + nq$ (R = *i*-Pr, *t*-Bu, Ph) (Eq. (1)).

olefin-free Pd(0) species [Pd(SNS(R))], possibly also containing a coordinated solvent molecule. Consistently, no independent k_1 paths have been observed in earlier works in which Pd(0) complexes with bidentate NS ligands were examined [6].

The fact that the k_1 term appears to be virtually insensitive to the R substituent in the chelating ligand might be taken as an indication that the k_1 pathway is dissociative in nature. However, the k_1 term in rate law Eq. (1) could not be detected for SNS(R) (R = Me, Et) and NSN complexes. In the case of R = Me, extensive decomposition prevents any measurement. In the case of R = Et, the determination is plagued by a high uncertainty due to decomposition side reactions. The lack of a reliably measurable k_1 term for the NSN complex may be ascribed to the low tendency of this ligand to behave as terdentate due to the unfavorable position of the dangling pyridine nitrogen caused by the tetrahedral sulfur hybridization. On the other hand the k_2 values in Table 2 parallel those obtained under similar conditions in analogous reactions involving the mentioned bidentate ligands as far as both the magnitude and the adverse effect of the steric demands of the R group are concerned. The latter confirms the associative nature of the direct olefin exchange pathway (k_2) under study. A reasonable value for k_2 in the case of [Pd(η²-nq)(SNS(Me))] reacting with tmetc can be deduced by extrapolating the LFER plot of log k_2 versus the Beckhaus front strain parameter [9] for the R substituent on the SNS(R) ligand, which has proved useful in analyzing analogous associative olefin exchanges. The k_2 value for R = Ph arises apparently from a balance of steric and favorable electronic effects which renders this group comparable to the *i*-Pr sub-

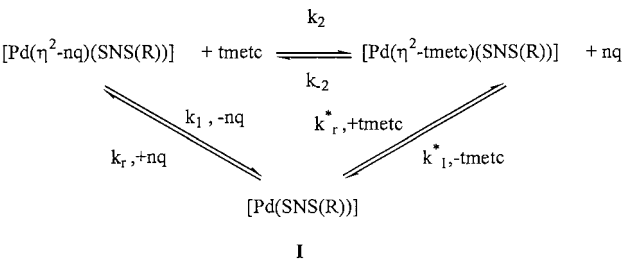

Scheme 2.

Table 2
First and second order rate constants for olefin exchange reactions with tmetc in $CHCl_3$ at 25°C

Complex	k_1 (s^{-1})	k_2 ($dm^3\ mol^{-1}\ s^{-1}$)
[Pd(η²-nq)(SNS(Me))]		33 [a]
[Pd(η²-nq)(SNS(Et))]		9 ± 2
[Pd(η²-nq)(SNS(*i*-Pr))]	$3.8 \times 10^{-4} \pm 4 \times 10^{-5}$	0.68 ± 0.01
[Pd(η²-nq)(SNS(*t*-Bu))]	$4.1 \times 10^{-4} \pm 3 \times 10^{-5}$	0.074 ± 0.004
[Pd(η²-nq)(SNS(Ph))]	$1.2 \times 10^{-3} \pm 1 \times 10^{-3}$	0.9 ± 0.1
[Pd(η²-nq)(NSN)]		15.3 ± 0.4

[a] Extrapolated value from the linear regression of log k_2 versus S (Beckhaus Front Strain parameter) see text.

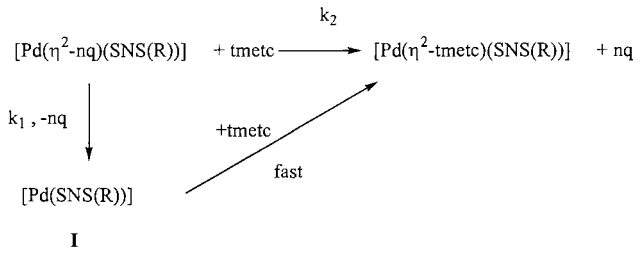

Scheme 3.

stituent. Fig. 2 shows the LFER plot of log k_2 versus the front strain parameter of R for SNS(R) ligands [6b].

We have also studied kinetically the approach to equilibrium for the reaction

$$[Pd(\eta^2 - nq)(SNS(i-Pr))] + tmetc \underset{k_{-2}}{\overset{k_2}{\rightleftharpoons}} [Pd(\eta^2 - tmetc)(SNS(i-Pr))] + nq \quad (3)$$

by the use of an excess of both reacting olefins, tmetc and nq, where upon the equilibria involving the olefin-free intermediate **I** are suppressed ($[Pd]_0 = 1 \times 10^{-4}$, $[tmetc] = 1.04 \times 10^{-3}$–$4.04 \times 10^{-3}$, $[nq]_0 = 1.3 \times 10^{-3}$ mol dm^{-3}, $\lambda = 410$ nm). Under these conditions the pseudo first-order rate constants k_{obs} fit the linear relationship (Fig. 3)

$$k_{obs} = k_{-2}[nq]_0 + k_2[tmetc] \quad (4)$$

The k_2 and k_{-2} values obtained by linear regression according to Eq. (4) are 0.71 ± 0.04 and 1.61 ± 0.02 mol^{-1} dm^3 s^{-1}, respectively. The resulting k_2 parameter is in very good agreement with the value reported in Table 2 which was determined from Eq. (1). The ratio $k_2/k_{-2} = K_{equil}$ (0.44 ± 0.03) is close to unity, similar to those measured in the analogous way for bidentate NS(R) ligands [6b]. This confirms earlier views that the two Pd(0)–olefin complexes involved in the exchange

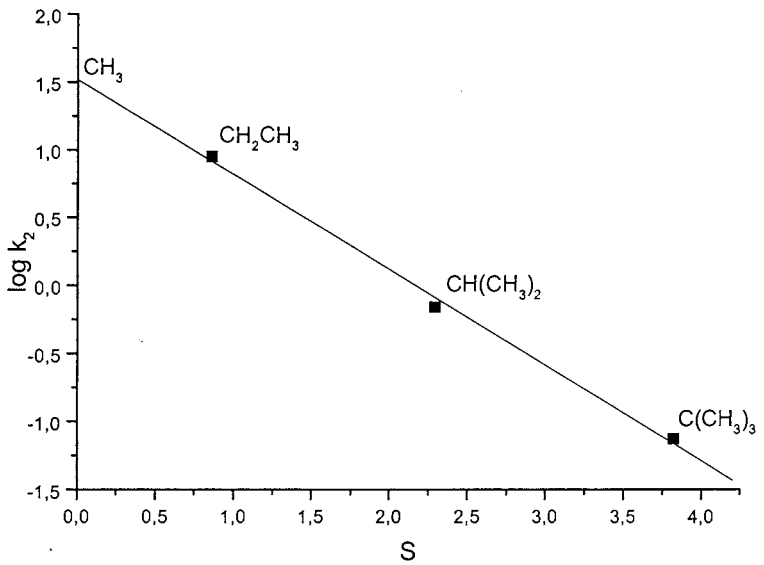

Fig. 2. LFER between log k_2 for alkyl-substituted ancillary ligand complexes and Beckhaus front strain parameter of R alkyl substituent.

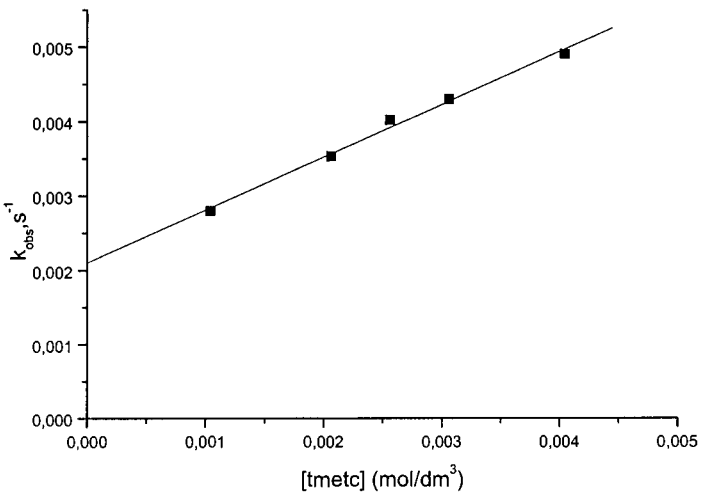

Fig. 3. Fit of k_{obs} to added tmetc concentration under pseudo-first order conditions for both direct and reverse paths of reaction (3).

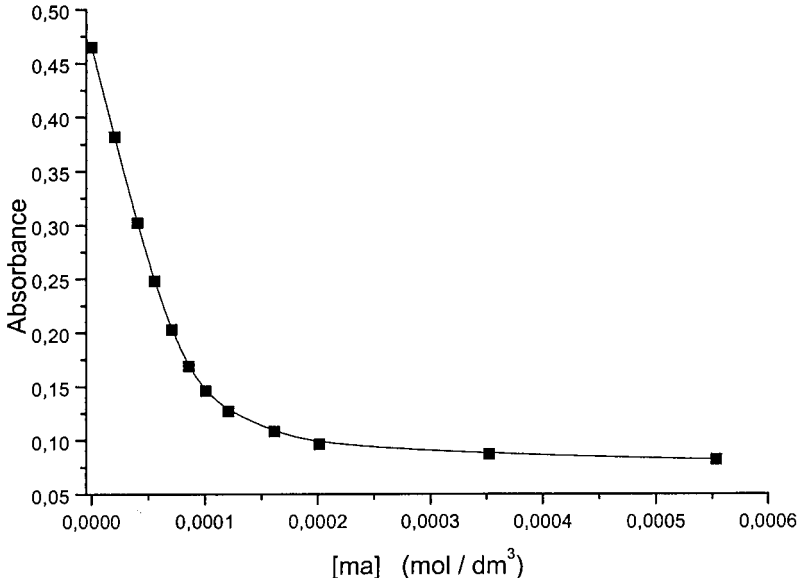

Fig. 4. Non-linear fit of absorbance to entering olefin concentration for K_E determination for reaction (5) in acetone at 298 K (R = *i*-Pr).

have similar stability as far as this is governed by the electron-withdrawing ability of the olefin substituents, with the bidentate or terdentate ligand hardly affecting this feature.

2.2. Olefin substitution equilibrium constants

Equilibrium constants for the reactions

$$[\underset{\mathbf{1}}{\text{Pd}(\eta^2-\text{nq})}(\text{LL}'\text{L})] + \text{ol} \overset{K_E}{\rightleftharpoons} [\underset{\mathbf{2}}{\text{Pd}(\eta^2-\text{ol})}(\text{LL}'\text{L})] + \text{nq} \quad \text{where LL'L} = \text{SNS(R)},\ \text{ol} = \text{ma or NSN},\ \text{ol} = \text{ma, fn} \tag{5}$$

in $CHCl_3$ or acetone were determined by recording spectral changes in the range 300–600 nm of mixtures obtained by adding appropriate microaliquots of solutions of ol to a solution of **1** ($[Pd]_0$ ca. 1×10^{-4} mol dm^{-3}) in the thermostatted cell compartment of the spectrophotometer. Acetone was also chosen as the solvent since in $CHCl_3$ decomposition takes place in some cases. The equilibria were rapidly established. Absorbance data were analyzed at 410 nm in the case of SNS(R) derivatives and at 400 nm in the case of [Pd(η^2-nq)(SNS)] complex where the change in absorbance was the largest and the olefins ol and nq do not absorb appreciably.

Under these conditions abstract factor analysis [10] of the observed spectral changes indicated that at most two independently absorbing species were present, i.e. complexes **1** and **2**.The absorbance data D_λ were fitted by non-linear least squares according to the model

$$K_E = [\mathbf{2}][\text{nq}]/[\mathbf{1}][\text{ol}]$$

$$[\text{Pd}]_{\text{tot}} = [\mathbf{1}] + [\mathbf{2}]$$

$$[\text{nq}] + [\text{ol}] = [\text{nq}]_0 + [\text{ol}]_0$$

$$[\text{nq}] = [\text{nq}]_0 + [\mathbf{2}]$$

$$D_\lambda = \varepsilon_1[\mathbf{1}] + \varepsilon_2[\mathbf{2}]$$

The parameters to be optimized were K_E and ε_2.The latter was either held constant at the experimentally accessible value (from the spectrum of complex **2** independently prepared) or allowed to float during the iterative process. In the latter case, the final optimized value turned out to coincide with that determined directly (Fig. 4). The K_E values are also listed in Table 3.

As can be seen, the K_E values in both solvents cover a narrow range, spanning at most one order of magnitude. The complexes in acetone appear to be somewhat leveled off. The complexes with ma are in general more stable ($K_E > 1$) than those of nq, thanks to the higher electron-withdrawing ability of the former olefin. This behavior is in agreement with our previous findings

Table 3
Equilibrium constant (K_E) for the reaction (5) at 25°C in $CHCl_3$

Complex	K_E [a] in CH_3COCH_3	K_E [a] in $CHCl_3$
[Pd(η^2-nq)(SNS(Me))]	4.9 ± 0.2	Decomposition
[Pd(η^2-nq)(SNS(Et))]	5.2 ± 0.3	11.5 ± 0.6
[Pd(η^2-nq)(SNS(*i*-Pr))]	13.1 ± 0.5	22 ± 3
[Pd(η^2-nq)(SNS(*t*-Bu))]	14 ± 1	53 ± 2
[Pd(η^2-nq)(SNS(Ph))]	7.2 ± 0.2	Decomposition
	Entering olefin	
[Pd(η^2-nq)(NSN)]	ma	11 ± 2
	fn	3.5 ± 0.5

[a] Entering olefin: ma.

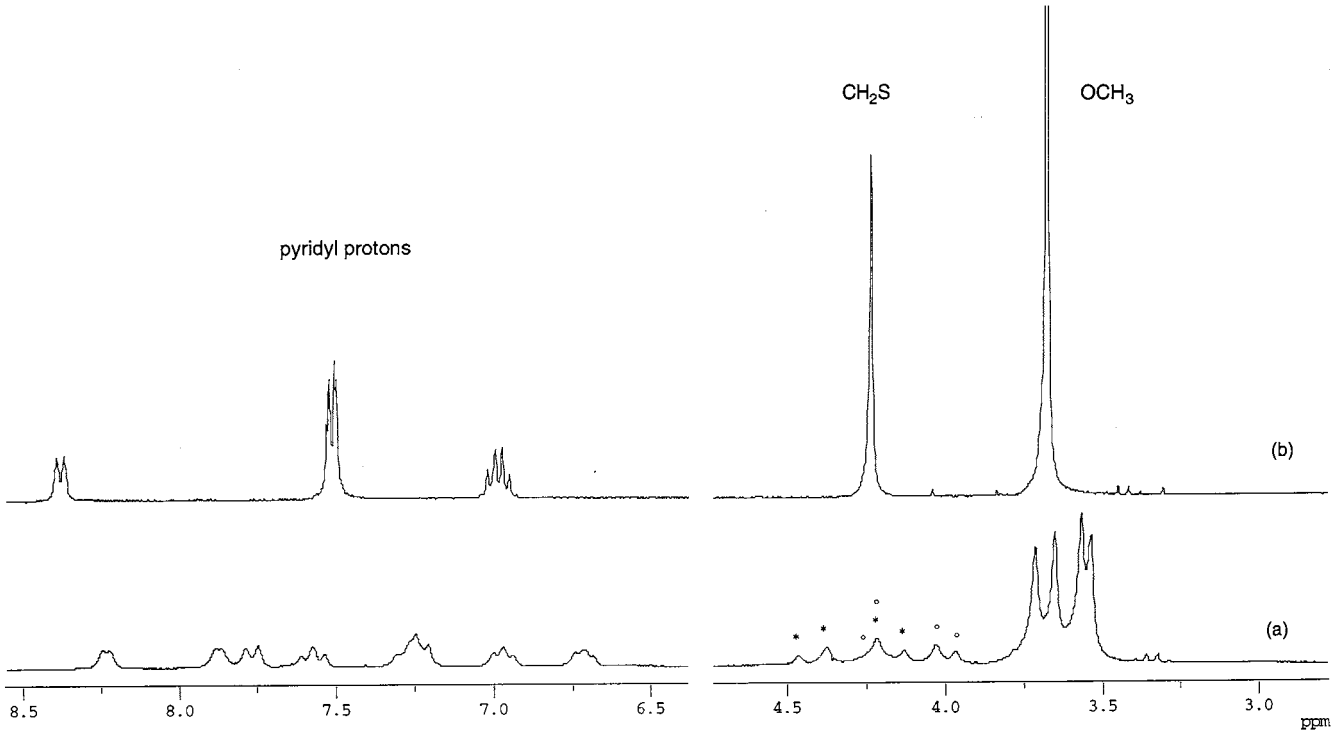

Fig. 5. ^{1}H-NMR spectra of [Pd(η^2-tmetc)(NSN)] at 178 (5a) and 298 K (5b) in $CDCl_3$.

about olefin exchange in Pd(0) complexes with α-diimines and pyridinthioethers. The equilibrium constants for terdentate ligand complexes are fairly close to those for exchange of the same olefins in analogous bidentate systems, indicating that the governing factor affecting the thermodynamic stability of these Pd(0) olefin complexes is the relative electron-withdrawing properties of the olefins involved, the nature and potential behavior of the chelating ancillary ligands playing only a minor role.

These findings were confirmed also in the case of the [Pd(η^2-nq)(NSN)] complex. The olefin exchange equilibria were determined in this case only in $CHCl_3$, thanks to the stability of the substrate, using ma and fn as entering olefins (Table 3). The values of K_E confirm that maleic anhydride is the more stabilizing olefin.

3. NMR studies

3.1. Characterization of complexes and fluxional behavior

Selected ^{1}H- and ^{13}C-NMR spectral data for the complexes under study are reported in the Section 4.

The room temperature ^{1}H-NMR spectra of the complexes display features typical of symmetric species, which are inconsistent with the presence of a terdentate species acting as a bidentate ' arm off ' ligand and an olefin in a square-planar environment. These observations could be better explained by invoking a fluxional behavior in which the symmetry arises from fast (on the NMR time scale) alternating 'windscreen wipe' motion of the two wings bearing the peripheral nucleophiles. This phenomenon has already been observed in Pd(II) η^3-allyl complexes in which potentially terdentate ligands display similar behavior [5g]. This hypothesis is confirmed by the analysis of variable temperature spectra of the most diagnostic complex [Pd(η^2-tmetc)(NSN)]. The spectrum at 178 K shows an asymmetry, which can only be ascribed to a bidentate NS species with a dangling pyridine arm. In fact, the spectrum at this temperature displays four singlets (3.72, 3.66, 3.58, 3.55 ppm), a multiplet at 4.22 ppm, and seven signal groups in the aromatic range (Fig. 5(a)). The latter are easily interpreted as eight signals ascribable pair wise to the four protons of the coordinated pyridine (lower field) and to those of the uncoordinated pyridine (higher field). The 4.22 ppm multiplet is made up of two partially overlapping AB quartets ascribed to the thiomethyl CH_2–S protons belonging to the two arms differently engaged in the coordination to the metal (i.e. coordinated and uncoordinated wing). The presence of two AB systems also implies the freezing of pyramidal sulfur inversion [6b]. The asymmetry in the complex brings about a difference in the chemical environments of olefin substituents which place themselves at the right and the left of a plane perpendicular to the main coordination plane and above and below the coordination plane with respect to the substituent

moiety (–CH_2–pyridine) of the frozen sp^3 sulfur. This will explain the presence of the four singlets ascribable to the olefinic carbomethoxy protons. On increasing the temperature, rapid flipping involving both pyridine-bearing arms induces an increasing generalized symmetry, as can be seen from the 298 K ^{1}H-NMR spectrum (Fig. 5(b)). In fact, the four high field carbomethoxy singlets collapse into a singlet (3.68 ppm). Meanwhile simplification of the two AB systems ascribable to the –CH_2–pyridine protons into a singlet (4.24 ppm) and formation of a unique pyridine ABXY system in the aromatic region occurs (Fig. 5(b)).

This observed fluxional behavior does not necessarily involve either sulfur inversion or olefin propeller-like rotation. In fact, rotation of the bulky olefin tmetc seems to be severely hindered in related bidentate NS complexes [11].

The complexes [Pd(η^2-tmetc)(SNS)(R)] display analogous fluxional features arising from the fast alternating flipping of the sulfur-bearing arms, although analysis of the variable temperature spectra is not as diagnostic as that of the NSN analog [Pd(η^2-tmetc)(NSN)] due to the much lower, unattainable freezing temperature. This can be explained by the better ability of sulfur as compared to nitrogen as a nucleophile and/or by the lesser strain required by the SNS ligand to act as terdentate. However in the case of the complex [Pd(η^2-tmetc)(SNS(Ph))], the fluxional movement is clearly depressed at low temperature. In fact, at 178 K the presence of a singlet due to the CH_2–S protons of uncoordinated arm (4.56 ppm) superimposed to a broad AB system due to the CH_2–S protons of the coordinated one is observed. Moreover the high field spectrum displays a broad signal due to the olefin carbomethoxy protons in which two separated singlets (3.57 ppm, 3H; 3.31ppm, 3H) and an unresolved one (3.61 ppm, 6H) are identified. The ' wind-screen ' movement is readily restored on slightly increasing the temperature (183 K), as can be deduced from the collapse of the signals.

3.2. Olefin exchange reactions between palladium(0) complexes

We sought to confirm the hypothesis of an olefin dissociative pathway in the olefin exchange reactions studied kinetically (Eq. (1)) by carrying out a crossover experiment involving an equimolar mixture ($[Pd]_0 = 2 \times 10^{-2}$ mol dm^{-3}) of [Pd(η^2-tmetc)(SNS (Et))] and [Pd(η^2-ma)(SNS(*i*-Pr))] in $CDCl_3$ at 25°C. The ability of at least one of these complexes to release its coordinated olefin by a dissociative path should lead to the establishment of an equilibrium involving the presence of all four species, i.e. the starting substrates and the olefin exchange products [Pd(η^2-tmetc)(SNS(*i*-Pr))] and [Pd(η^2-ma)(SNS(Et))] which can only be detected if the rate of olefin exchange is slow on the NMR time scale. In fact, the ^{1}H-NMR spectrum of the reaction mixture displays signals ascribable to all four species involved. Apparently, the less efficient tmetc is ideally suited for this type of experiment. As expected, the same equilibrium composition can be attained by mixing equimolar amounts of the final exchange products. Analogous results were obtained with those other complexes that display a dissociative term in the rate law (Eq. (1)). Needless to say, the merit of this experiment rests on the absence of other causes of exchange, such as direct binuclear bimolecular olefin or polydentate ligand exchange or sufficient decomposition to allow a significant concentration of free olefin in the mixture (i.e. no formation of metallic palladium was observed). The most we can say is that the latter occurrence can be safely ruled out. A similar crossover experiment was devised by Elsevier et al. to provide evidence for an olefin dissociative mechanism in Pd(0) olefin complexes containing rigid bidentate ligands [7a]. The possibility of a binuclear second-order path was in that case ruled out on steric grounds.

3.3. Allyl complexes

Since it was not possible to prepare some Pd(0) species by direct exchange reactions of the appropriate ligand and olefin with $Pd_2(dba)_3{\cdot}CHCl_3$ (see Table 1), we devised to synthesize the fn derivative [Pd(η^2-fn)(SNS(*t*-Bu))] by amination of [Pd(η^3-allyl)(SNS(*t*-Bu))]SO_3CF_3 with piperidine in the presence of fn ([4a,b] and Refs. therein).

The fluxional behavior of the parent η^3-allyl complex is similar to that of its SNS(Me) analogs containing either η^3-C_3H_5 or η^3-1,1-$Me_2C_3H_3$, in which the alternating flipping movement of the arms induces a η^3–η^1 allyl isomerization [5f,g]. It is worth noting that the NSN analog [Pd(η^3-allyl)(NSN)]$^+$, while undergoing the fast flipping movement of the potentially terdentate ligand, does not induce any η^3–η^1 rearrangement of the allyl fragment, probably owing to the lower coordinating ability of the nitrogen relative to sulfur combined with a higher strain involved in the chelate rings when NSN acts as terdentate (vide supra).

The amination of the complex [Pd(η^3-allyl)(SNS(*t*-Bu))]$^+$ by piperidine was followed at 25°C in $CDCl_3$ either in the presence or in the absence of fn ($[Pd]_0 = 0.05$, $[fn]_0 = 0.05$, $[pip]_0 = 0.25$ mol dm^{-3}). The reaction in the presence of fn is easily interpreted on the basis of the characteristic spectral features of [Pd(η^2-fn)(SNS(*t*-Bu))] and the allylamine $C_5H_{10}N$–$CH_2CH{=}CH_2$ (see Section 4). In the absence of fn, the reaction takes place with formation of allylamine but is accompanied by extensive decomposition, as indicated by the presence of free polydentate ligand. However, there is spectral evidence at low fields in the pyridine protons range for

formation of a Pd(0) species which is most likely identified as the terdentate olefin-free [Pd(SNS(*t*-Bu))]. This observation, coupled to the kinetic findings discussed above, lends support to the view that sufficient Pd(0) stabilization by SNS ligands may occur even in the absence of a stabilizing π-accepting olefin.

4. Experimental

4.1. Preparation of ligands

4.1.1. 2[(2-Pyridylmethylthio)methyl)]pyridine (NSN)

The title compound was prepared as in Ref. [5g].

4.1.2. 2,6-bis(Methylthiomethyl)pyridine (SNS(Me))

The title compound was prepared as in Ref. [12].

4.1.3. 2,6-bis(Arylthiomethyl)pyridine (SNS(R))

These compounds were prepared in a way similar to (SNS(Me)) using the suitable thiolate RS^-K^+ (R = Et, *i*-Pr, *t*-Bu, Ph).

4.1.3.1. SNS(Et). Yield 74%. ^{1}H-NMR (in $CDCl_3$, RT), δ (ppm): H^4 7.62 (t, 1H, $J = 7.7$ Hz); $H^{3,5}$ 7.26 (d, 2H, $J = 7.7$ Hz); CH_2–S 3.83 (s, 4H); S–CH_2–CH_3 2.50 (q, 4H, $J = 7.5$ Hz); SCH_2CH_3 1.24 (t, 6H, $J = 7.5$ Hz). ^{13}C-NMR (in $CDCl_3$, RT), δ (ppm): C^4 137.2; $C^{3,5}$ 158.5; $C^{2,6}$ 120.9; CH_2–S 37.7; S–CH_2CH_3 25.6; SCH_2CH_3 14.4.

4.1.3.2. SNS(i-Pr). Yield 99%. ^{1}H-NMR (in $CDCl_3$, RT), δ (ppm): H^4 7.56 (t, 1H, $J = 7.7$ Hz); $H^{3,5}$ 7.23 (d, 2H, $J = 7.7$ Hz); CH_2–S 3.81 (s, 4H); S–C$H(CH_3)_2$ 2.84 (sept, 2H, $J = 6.7$ Hz); S–CH(CH_3)$_2$ 1.19 (d, 12H, $J = 6.7$ Hz). ^{13}C-NMR (in $CDCl_3$, RT), δ (ppm): C^4 137.1; $C^{3,5}$ 158.5; $C^{2,6}$ 120.9; CH_2–S 37.0; S–CH 34.6; S–CH(CH_3)$_2$ 23.2.

4.1.3.3. SNS(t-Bu). Yield 94%. ^{1}H-NMR (in $CDCl_3$, RT), δ (ppm): H^4 7.58 (t, 1H, $J = 7.7$ Hz); $H^{3,5}$ 7.32 (d, 2H, $J = 7.7$ Hz); CH_2–S 3.91 (s, 4H); S–C$(CH_3)_3$ 1.34 (s, 18H). ^{13}C-NMR (in $CDCl_3$, RT), δ (ppm): C^4 136.9; $C^{3,5}$ 158.5; $C^{2,6}$ 121.2; CH_2–S 43.1; S–$C(CH_3)_3$ 35.5; $SC(CH_3)_3$ 31.0.

4.1.3.4. SNS(Ph). Yield 67%. ^{1}H-NMR (in $CDCl_3$, RT), δ (ppm): H^4 7.51 (t, 1H, $J = 7.7$ Hz); CH_2–S 4.26 (s, 4H); $H^{3,5}$ Phenyl protons 7.25 (m, 12H). ^{13}C-NMR (in $CDCl_3$, RT), δ (ppm): C^4 137.2; $C^{3,5}$ 157.3; $C^{2,6}$ 121.2; C^a 135.8; C^b 129.5; C^c 120.9; C^d 126.3; CH_2–S 40.3.

4.2. Preparation of [Pd(η^3-C_3H_5)(SNS(*t*-Bu))]SO_3CF_3

To a solution of 0.087 g (0.238 mmol) of [Pd(η^3-C_3H_5)Cl]$_2$ in 10 ml of freshly distilled $CHCl_3$, 0.124 g (0.483 mmol) of Ag SO_3CF_3 were added under inert atmosphere (N_2). The resulting solution was stirred in the dark for 4 h. To the filtered solution (glass-fiber filter) 0.141 g (0.497 mmol) of 2,6-bis-(*t*-butylthiomethyl)pyridine (SNS(*t*-Bu)) was added. The solution was stirred for 1 h, treated with activated charcoal for 15 min and filtered on celite filter. Addition of diethylether to the concentrated solution yields 0.229 g (0.395 mmol, yield 83%) of the title complex as a white precipitate. Anal. Found: C, 39.46; H, 5.17; N, 2.36. $C_{19}H_{30}NO_3S_3F_3Pd$ requires: C, 39.34; H, 5.21; N, 2.41%. The following numbering scheme was used for the allylic fragment:

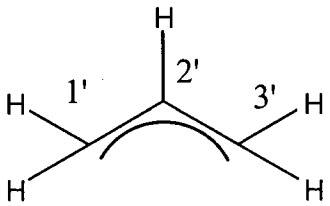

IR (in KBr, cm^{-1}): $\nu_{C=N}$ 1598 (m); $\nu_{S=O}$ 1269 (s). ^{1}H-NMR (in $CDCl_3$, RT), δ (ppm): H^4 7.89 (t, 1H, $J = 7.7$ Hz); $H^{3,5}$ 7.64 (d, 2H, $J = 7.7$ Hz); CH_2–S 4.40 (s, 4H); $SC(CH_3)_3$ 1.38 (s, 18H); $H^{1',3'}$ 4.05 (s, 4H, br); $H^{2'}$ 5.79 (qn, 1H, $J = 10.0$ Hz). ^{13}C{^{1}H}-NMR (in $CDCl_3$, RT), δ (ppm): $C^{2,6}$ 159.6; C^4 140.1; $C^{3,5}$ 123.1; $C^{2'}$ 120.9; $C^{1',3'}$ 65.8; CH_2–S 40.5; S–$C(CH_3)_3$ 48.8; S–C(CH_3)$_3$ 30.4.

4.3. Preparation of Pd(0) complexes

4.3.1. $Pd_2(dba)_3 \cdot CHCl_3$

The title complex was obtained according to Ref. [13].

4.3.2. [Pd(η^2-ol)(LL′L)]

The published complexes [Pd(η^2-fn)(SNS(Me))], [Pd(η^2-fn)(NSN)] and the following reported species were obtained according to Ref. [5g].

The following numbering scheme was adopted:

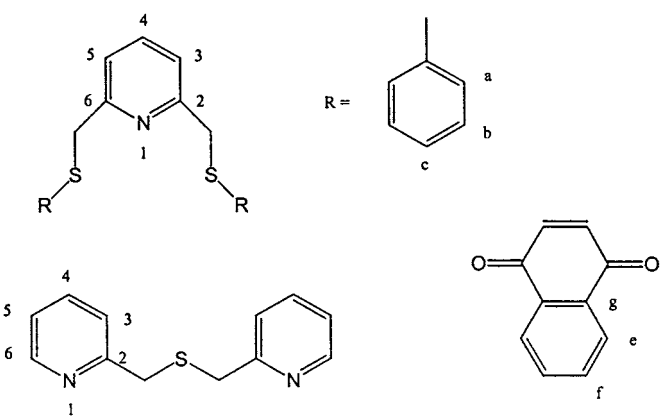

4.3.3. [Pd(η²-ma)(SNS(Me))]

Yield 87% (yellow microcrystals). Found: C, 38.64; H, 3.81; N, 3.51. $C_{13}H_{15}NO_3S_2Pd$ requires: C, 38.71; H, 3.75; N, 3.48%. IR (in KBr, cm^{-1}): $\nu_{C=O}$ 1788 (s), 1713 (s); $\nu_{C=N}$ 1593 (m). ^{1}H-NMR (in $CDCl_3$, RT), δ (ppm): H^4 7.80 (t, 1H, $J = 7.7$ Hz); $H^{3,5}$ 7.42 (d, 2H, $J = 7.7$ Hz); CH_2–S and HC=CH 4.16 (s, 6H); S–CH_3 2.24 (s, 6H). $^{13}C\{^1H\}$-NMR (in CD_2Cl_2, RT), δ (ppm): C^4 137.8; $C^{3,5}$ 122.1; $C^{2,6}$ 158.3; C=O 170.8; CH_2–S 43.6; S–CH_3 16.6; HC=CH 44.5.

4.3.4. [Pd(η²-ma)(SNS(Et))]

Yield 88% (yellow microcrystals). IR (in KBr, cm^{-1}): $\nu_{C=O}$ 1794 (s), 1715 (s); $\nu_{C=N}$ 1593 (m). ^{1}H-NMR (in $CDCl_3$, RT), δ (ppm): H^4 7.78 (t, 1H, $J = 7.7$ Hz); $H^{3,5}$ 7.41 (d, 2H, $J = 7.7$ Hz); CH_2–S and HC=CH 4.19 (s, 6H); S–CH_2CH_3 2.67 (q, 4H, $J = 7.4$ Hz); SCH_2CH_3 1.31 (t, 6H, $J = 7.4$ Hz). $^{13}C\{^1H\}$-NMR (in CD_2Cl_2, RT), δ (ppm): C^4 137.7; $C^{3,5}$ 121.8; $C^{2,6}$ 158.7; C=O 170.9; CH_2–S 41.5; S–CH_2CH_3 27.6; SCH_2CH_3 13.4; HC=CH 44.3.

4.3.5. [Pd(η²-ma)(SNS(i-Pr))]

Yield 87% (yellow microcrystals). IR (in KBr, cm^{-1}): $\nu_{C=O}$ 1795 (s), 1724 (s); $\nu_{C=N}$ 1597 (m). ^{1}H-NMR (in $CDCl_3$, RT), δ (ppm): H^4 7.76 (t, 1H, $J = 7.7$ Hz); $H^{3,5}$ 7.42 (d, 2H, $J = 7.7$ Hz); CH_2–S and HC=CH 4.20 (s, 6H); S–$CH(CH_3)_2$ 3.00 (sept, 2H, $J = 6.7$ Hz); $SCH(CH_3)_2$ 1.34 (d, 12H, $J = 6.7$ Hz). $^{13}C\{^1H\}$-NMR (in CD_2Cl_2, RT), δ (ppm): C^4 137.7; $C^{3,5}$ 121.7; $C^{2,6}$ 159.0; C=O 171.0; CH_2–S 40.5; S–$CH(CH_3)_2$ 37.0; $SCH(CH_3)_2$ 22.1; HC=CH 44.2.

4.3.6. [Pd(η²-ma)(SNS(t-Bu))]

Yield 70% (yellow microcrystals). Found: C, 46.77; H, 5.61; N, 2.91. $C_{19}H_{27}NO_3S_2Pd$ requires: C, 46.81; H, 5.59; N, 2.88%. IR (in KBr, cm^{-1}): $\nu_{C=O}$ 1795 (s), 1724 (s); $\nu_{C=N}$ 1597 (m). ^{1}H-NMR (in $CDCl_3$, RT), δ (ppm): H^4 7.75 (t, 1H, $J = 7.7$ Hz); $H^{3,5}$ 7.46 (d, 2H, $J = 7.7$ Hz); CH_2–S e HC=CH 4.22 (s, 6H); $SC(CH_3)_3$ 1.42 (s, 18H). $^{13}C\{^1H\}$-NMR (in CD_2Cl_2, RT), δ (ppm): C^4 138.1; $C^{3,5}$ 122.2; $C^{2,6}$ 159.8; C=O 171.7; CH_2–S 39.2; S–$C(CH_3)_3$ 46.0; $SC(CH_3)_3$ 30.5; HC=CH 45.2.

4.3.7. [Pd(η²-ma)(SNS(Ph))]

Yield 95% (yellow microcrystals). Found: C, 52.42; H, 3.58; N, 2.69. $C_{23}H_{19}NO_3S_2Pd$ requires: C, 52.37; H, 3.63; N, 2.66%. IR (in KBr, cm^{-1}): $\nu_{C=O}$ 1796 (s), 1724 (s); $\nu_{C=N}$ 1593 (m). ^{1}H-NMR (in $CDCl_3$, RT), δ (ppm): H^4 7.58 (t, 1H, $J = 7.7$ Hz); CH_2–S 4.49 (s, 4H); HC=CH 4.27 (s, 2H); $H^{3,5}$, H^b, H^c, H^d, 7.25 (m, 12H). $^{13}C\{^1H\}$-NMR (in $CDCl_3$, RT), δ (ppm): C^4 138.0; $C^{3,5}$ 122.5; $C^{2,6}$ 158.3; C=O 171.5; C^a 132.6; C^b 131.5; C^c 129.0; C^d 128.1; CH_2–S 46.1.

4.3.8. [Pd(η²-ma)(NSN)]

Yield 95% (yellow microcrystals). Found: C, 45.58; H, 3.38; N, 6.69. $C_{16}H_{14}N_2O_3SPd$ requires: C, 45.72; H, 3.36; N, 6.67%. IR (in KBr, cm^{-1}): $\nu_{C=O}$ 1792 (s), 1724 (s); $\nu_{C=N}$ 1592 (m). ^{1}H-NMR (in $CDCl_3$, RT), δ (ppm): H^6 8.30 (d, 1H, $J = 5.2$ Hz); H^4 7.70 (td, 1H, $J = 7.7$, 1.6 Hz); H^3 7.46 (d, 1H, $J = 7.7$ Hz); H^5 7.09 (dd, 1H, $J = 7.7$, 5.2 Hz); CH_2–S 4.16 (s, 4H); HC=CH 4.16 (s, 2H). ^{13}C-NMR (in $CDCl_3$, RT), δ (ppm):C=O 171.6; C^2 156.8; C^6 150.3; C^4 137.5; C^5 123.6; C^3 122.8; C=C 46.0; CH_2–S 41.9.

4.3.9. [Pd(η²-nq)(SNS(Me))]

Yield 74% (brown–orange microcrystals). Found: C, 49.11; H, 4.12; N, 3.01. $C_{19}H_{19}NO_2S_2Pd$ requires: C, 49.19; H, 4.13; N, 3.02%. IR (in KBr, cm^{-1}): $\nu_{C=O}$ 1626;$\nu_{C=N}$ 1587 (m). ^{1}H-NMR (in $CDCl_3$, RT), δ (ppm): H^4 7.64 (t, 1H, $J = 7.6$ Hz); $H^{3,5}$ 7.21 (d, 2H, $J = 7.6$ Hz); CH_2–S 4.04 (s, 4H); S–CH_3 2.27 (s, 6H); HC=CH 4.65 (s, 2H, br); H^e 7.97 (m, 2H); H^f 7.52 (m, 2H). $^{13}C\{^1H\}$-NMR (in $CDCl_3$, RT), δ (ppm): C^4 138.0; $C^{3,5}$ 123.1; $C^{2,6}$ 160.0; C1=O 183.2; C^e 124.9; C^f 131.5; C^g 135.1; HC=CH 63.9; CH_2–S 44.6; S–CH_3 17.5.

4.3.10. [Pd(η²-nq)(SNS(Et))]

Yield 61% (brown–orange microcrystals). IR (in KBr, cm^{-1}): $\nu_{C=O}$ 1624 (s); $\nu_{C=N}$ 1587 (m). ^{1}H-NMR (in $CDCl_3$, RT), δ (ppm): H^4 7.66 (t, 1H, $J = 7.7$ Hz); $H^{3,5}$ 7.31 (d, 2H, $J = 7.7$ Hz); CH_2–S 4.09 (s, 4H); S–CH_2CH_3 2.62 (q, 4H, $J = 7.3$ Hz); SCH_2CH_3 1.22 (t, 6H, $J = 7.3$ Hz); HC=CH 4.87 (s, 2H, br); H^e 8.00 (m, 2H); H^f 7.54 (m, 2H). $^{13}C\{^1H\}$-NMR (in $CDCl_3$, RT), δ (ppm): C^4 137.9; $C^{3,5}$ 122.8; $C^{2,6}$ 158.5; C=O 183.9; C^e 125.0; C^f 131.5; C^g 134.9; C=C 63.2; CH_2–S 41.7; S–CH_2CH_3 28.3; S–CH_2CH_3 14.0.

4.3.11. [Pd(η²-nq)(SNS(i-Pr))]

Yield 79% (orange microcrystals). Found: C, 53.18; H, 5.10; N, 2.81. $C_{23}H_{27}NO_2S_2Pd$ requires: C, 53.13; H, 5.23; N, 2.69%. IR (in KBr, cm^{-1}): $\nu_{C=O}$ 1641 (s), 1616 (s); $\nu_{C=N}$ 1589 (m). ^{1}H-NMR (in $CDCl_3$, RT), δ (ppm): H^4 7.66 (t, 1H, $J = 7.7$ Hz); $H^{3,5}$ 7.31 (d, 2H, $J = 7.7$ Hz); CH_2–S 4.07 (s, 4H); S–$CH(CH_3)_2$ 2.90 (sept, 2H, $J = 6.6$ Hz); $SCH(CH_3)_2$ 1.27 (d, 12H, $J = 6.7$ Hz); HC=CH 4.89 (s, 2H, br); H^e 8.02 (m, 2H); H^f 7.48 (m, 2H). $^{13}C\{^1H\}$-NMR (in $CDCl_3$, RT), δ (ppm): C^4 137.7; $C^{3,5}$ 121.9; $C^{2,6}$ 159.6; C=O 185.0; C^e 125.0; C^f 131.1; C^g 135.3; HC=CH 60.7; CH_2–S 39.9; S–$CH(CH_3)_2$ 37.0; S–$CH(CH_3)_2$ 22.8.

4.3.12. [Pd(η²-nq)(SNS(t-Bu))]

Yield 60% (orange microcrystals). IR (in KBr, cm^{-1}): $\nu_{C=O}$ 1627 (s); $\nu_{C=N}$ 1591 (m). ^{1}H-NMR (in $CDCl_3$, RT), δ (ppm): H^4 7.64 (t, 1H, $J = 7.7$ Hz); $H^{3,5}$ 7.35 (d, 2H, $J = 7.7$ Hz); CH_2–S 4.14 (s, 4H); $SC(CH_3)_3$ 1.38 (s, 18H); HC=CH 4.88 (s, 2H); H^e 8.00 (m, 2H); H^f

7.47 (m, 2H). $^{13}C\{^1H\}$-NMR (in $CDCl_3$, RT), δ (ppm): C^4 137.7; $C^{3,5}$ 121.9; $C^{2,6}$ 160.1; C=O 185.7;C^e 125.0; C^f 131.0; C^g 135.5; HC=CH 60.7; CH_2–S 38.6; S–$C(CH_3)_3$ 45.8; S–C(CH_3)$_3$ 30.5.

4.3.13. [Pd(η^2-nq)(SNS(Ph))]

Yield 92% (brown–orange microcrystals). Found: C, 59.28; H, 3.89; N, 2.35. $C_{29}H_{23}NO_2S_2Pd$ requires: C, 59.23; H, 3.94; N, 2.38%. IR (in KBr, cm^{-1}): $\nu_{C=O}$ 1643 (s), 1620 (s); $\nu_{C=N}$ 1591 (m). ^{1}H-NMR (in $CDCl_3$, RT), δ (ppm): $H^{3,5}$ 7.04 (d, 2H, $J = 7.7$ Hz); CH_2–S 4.36 (s, 4H); HC=CH 4.96 (s, 2H); H^4, H^b, H^c, H^d, H^e, H^f 7.6 (m, 15H). $^{13}C\{^1H\}$-NMR (in $CDCl_3$, RT), δ (ppm): C^4 137.6; $C^{3,5}$ 122.4; $C^{2,6}$ 158.5; C=O 185.1; C^a 132.8; C^b 128.8; C^c 131.5; C^d 127.8; C^e 125.1; C^f 131.3; C^g 135.2; HC=CH 61.7; CH_2–S 45.3.

4.3.14. [Pd(η^2-nq)(NSN)]

Yield 83% (dark orange microcrystals). Found: C, 55.01; H, 3.81; N, 5.81. $C_{22}H_{18}N_2O_2SPd$ requires: C, 54.95; H, 3.77; N, 5.83%. IR (in KBr, cm^{-1}): $\nu_{C=O}$ 1626 (s); $\nu_{C=N}$ 1583 (m). ^{1}H-NMR (in $CDCl_3$, RT), δ (ppm): H^6, H^e 8.10 (m, 4H); H^f 7.55 (m, 2H); H^4 7.34 (td, 2H, $J = 7.7$, 1.6 Hz); H^3, H^5 7.00 (m, 4H); HC=CH 4.95 (s, 2H); CH_2–S 3.98 (s, 4H). $^{13}C\{^1H\}$-NMR (in $CDCl_3$, RT), δ (ppm): C^2 156.9; C^3 122.6; C^4 136.9; C^5 123.2; C^6 148.8; C=O 181.5; C^e 125.0; C^f 131.2; C^g 135.8; HC=CH 64.7; CH_2–S 40.8.

4.3.15. [Pd(η^2-tmetc)(SNS(Et))]

Yield 76% (yellow microcrystals). Found: C, 42.52; H, 4.89; N, 2.25. $C_{21}H_{29}NO_8S_2Pd$ requires: C, 42.46; H, 4.92; N, 2.36%. IR (in KBr, cm^{-1}): $\nu_{C=O}$ 1732 (s), 1689 (s); $\nu_{C=N}$ 1591 (m). ^{1}H-NMR (in $CDCl_3$, RT), δ (ppm): H^4 7.76 (t, 1H, $J = 7.7$ Hz); $H^{3,5}$ 7.52 (d, 2H, $J = 7.7$ Hz); CH_2–S 4.27 (s, 4H); O–CH_3 3.73 (s, 12H); S–CH_2CH$_3$ 2.65 (q, 4H, $J = 7.4$ Hz); SCH$_2$CH_3 1.27 (t, 6H, $J = 7.4$ Hz). $^{13}C\{^1H\}$-NMR (in CD_2Cl_2, RT), δ (ppm): C^4 140.3; $C^{3,5}$ 124.1; $C^{2,6}$ 161.6; C=O 171.3; O–CH_3 53.9; CH_2–S 43.6; S–CH_2CH_3 30.0; SCH$_2$CH_3 16.1; C=C not observed.

4.3.16. [Pd(η^2-tmetc)(SNS(i-Pr))]

Yield 77% (yellow microcrystals). IR (in KBr, cm^{-1}): $\nu_{C=O}$ 1724 (s), 1695 (s), 1674 (s); $\nu_{C=N}$ 1597 (m). ^{1}H-NMR (in $CDCl_3$, RT), δ (ppm): H^4 7.75 (t, 1H, $J = 7.7$ Hz); $H^{3,5}$ 7.52 (d, 2H, $J = 7.7$ Hz);CH_2–S 4.27 (s, 4H); O–CH_3 3.72 (s, 12H); S–CH(CH$_3$)$_2$ 2.90 (sept, 2H, $J = 6.7$ Hz); SCH(CH_3)$_2$ 1.30 (d, 12H, $J = 6.7$ Hz). $^{13}C\{^1H\}$-NMR (in $CDCl_3$, RT), δ (ppm): C^4 137.8; $C^{3,5}$ 121.6; $C^{2,6}$ 159.7; C=O 169.4; O–CH_3 52.0; CH_2–S 40.1; S–CH(CH$_3$)$_2$ 37.1; SCH(CH_3)$_2$ 22.8; C=C not observed.

4.3.17. [Pd(η^2-tmetc)(SNS(t-Bu))]

Yield 79% (yellow microcrystals). Found: C, 46.12; H, 5.81; N, 2.15. $C_{25}H_{37}NO_8S_2Pd$ requires: C, 46.19; H, 5.74; N, 2.15%. IR (in KBr, cm^{-1}): $\nu_{C=O}$ 1740 (s), 1720 (s), 1697 (s); $\nu_{C=N}$ 1598 (m). ^{1}H-NMR (in $CDCl_3$, RT), δ (ppm): H^4 7.73 (t, 1H, $J = 7.7$ Hz); $H^{3,5}$ 7.61 (d, 2H, $J = 7.7$ Hz); CH_2–S 4.25 (s, 4H); O–CH_3 3.72 (s, 12H); SC(CH$_3$)$_3$ 1.42 (s, 18H). $^{13}C\{^1H\}$-NMR (in CD_2Cl_2, RT), δ (ppm): C^4 137.6; $C^{3,5}$ 121.5; $C^{2,6}$ 160.2; C=O 169.5; O–CH_3 51.9; CH_2–S 38.8; S–C(CH$_3$)$_3$ 45.6; SC(CH_3)$_3$ 30.8; C=C not observed.

4.3.18. [Pd(η^2-tmetc)(SNS(Ph))]

Yield 79% (yellow microcrystals). Found: C, 50.51; H, 4.21; N, 2.05. $C_{29}H_{29}NO_8S_2Pd$ requires: C, 50.47; H, 4.24; N, 2.03%. IR (in KBr, cm^{-1}): $\nu_{C=O}$ 1720 (s), 1711 (s), 1680 (s); $\nu_{C=N}$ 1597 (m). ^{1}H-NMR (in $CDCl_3$, RT), δ (ppm): H^4 7.54 (t, 1H, $J = 7.7$ Hz); CH_2–S 4.62 (s, 4H); O–CH_3 3.66 (s, 12H); $H^{3,5}$, H^b, H^c, H^d 7.32 (m, 12H). $^{13}C\{^1H\}$-NMR (in $CDCl_3$, RT), δ (ppm): C^4 137.9; $C^{3,5}$ 121.9; $C^{2,6}$ 158.5; C=O 169.2; C^a 133.1; C^b 130.5; C^c 128.8; C^d 127.3; O–CH_3 52.1; CH_2–S 44.5; C=C not observed.

4.3.19. [Pd(η^2-tmetc)(NSN)]

Yield 85% (yellow microcrystals). Found: C, 45.41; H, 4.11; N, 4.85. $C_{22}H_{24}N_2O_8SPd$ requires: C, 45.33; H, 4.15; N, 4.81%. IR (in KBr, cm^{-1}): $\nu_{C=O}$ 1728 (s), 1695 (s); $\nu_{C=N}$ 1590 (m). ^{1}H-NMR (in $CDCl_3$, RT), δ (ppm): H^6 8.40 (d, 2H, $J = 5.0$ Hz); H^4, H^3 7.52 (m, 4H); H^5 6.96 (ddd, 2H, $J = 7.7$, 5.0, 1.8 Hz); CH_2–S 4.26 (s, 4H); O–CH_3 3.76 (s, 12H). $^{13}C\{^1H\}$-NMR (in $CDCl_3$, RT), δ (ppm): C^2 157.4; C^3 122.3; C^4 136.8; C^5 124.0; C^6 150.2; C=O 169.3; CH_2–S 41.0; O–CH_3 52.0; C=C not observed.

4.3.20. [Pd(η^2-fn)(SNS(Et))]

Yield 40% (white microcrystals) IR (in KBr, cm − 1): ν_{CN} 2202.6 (s), $\nu_{C=N}$ 1599 (m). ^{1}H-NMR (in $CDCl_3$, RT), δ (ppm): H^4 7.83 (t, 1H, $J = 7.7$ Hz); $H^{3,5}$ 7.48 (d, 2H, $J = 7.7$Hz); CH_2–S 4.28 (s, 4H); S–CH_2–CH$_3$ 2.73 (q, 4H, $J = 7.4$Hz); S–CH$_2$–CH_3 1.35 (t, 6H, $J =$ 7.4Hz); HC=CH 3.12 (s, 2H).

4.3.21. [Pd(η^2-fn)(SNS(t-Bu))]

The title complex was obtained in an NMR tube as the product of the amination reaction of [Pd(η^3-C_3H_5)(SNS(t-Bu))]SO_3CF_3 with piperidine (Pip) in the presence of fumaronitrile (fn) and was not separated.

In a typical experiment the complex [Pd(η^3-C_3H_5)(SNS(t-Bu))]SO_3CF_3, piperidine,and fumaronitrile ($[Pd]_0 = [fn]_0 = 5.10^{-2}$; $[Pip]_0 = 0.25$ mol dm^{-3}) were dissolved in 0.6 ml of $CDCl_3$. The reaction went to completion in a few minutes and the ^{1}H-NMR spectrum displays the signals ascribable to allylpiperidine (C_3H_5–NC_5H_{10}) [14] and to [Pd(η^2-fn)(SNS(t-Bu))] species.

^{1}H-NMR (in CDCl3, RT), δ (ppm): H^4 7.76 (t, 1H, $J = 7.7$Hz); $H^{3,5}$ 7.48 (d, 2H, $J = 7.7$Hz); CH_2–S 4.19,

4.33 (AB, 2H, $J = 15$Hz); HC=CH 3.12 (s, 2H); S–C(CH_3)$_3$ 1.40, (s, 18H).

4.4. IR and NMR measurements

The IR, ^{1}H, and ^{13}C{^{1}H}-NMR spectra were recorded on a Nicolet Magna™ 750 spectrophotometer and on a Bruker AC™ 200 spectrometer, respectively.

The temperature dependent ^{1}H-NMR spectra were analyzed using the SWAN program [15].

4.5. Kinetic and equilibrium measurements

The kinetics of olefin substitution were studied by addition of known aliquots of tmetc solutions to solutions of the complex under study in $CHCl_3$ ($[Pd]_0 \approx 10^{-4}$mol dm^{-3}) in the thermostatted cell compartment of a Lambda 40 Perkin–Elmer™ spectrophotometer at the designed temperature. The reactions were followed by recording spectral changes in the wavelength range of 300–540 nm or at a suitable fixed wavelength.

Equilibrium studies were performed by addition of microaliquots of a solution of the designed olefin (or ligand) to a solution of the complex under study at controlled temperature (25°C). The spectral features of the resulting mixtures were recorded by means of a Lambda 40 Perkin–Elmer spectrophotometer. Mathematical and statistical data analysis was carried out on a personal computer equipped with a locally adapted version of Marquardt's algorithm [16] written in Turbobasic™ (Borland).

References

[1] (a) F. Diederich, P.J. Stang, in: F. Diederich, P.J. Stang (Eds), Metal-Catalyzed Cross-Coupling Reactions, Wiley-VCH, Weinheim, (1998). (b) M.J. Calhorda, J.M. Brown, N.A. Cooley, Organometallics 10 (1991) 1431. (c) K. Selvakumar, M. Valentini, P.S. Pregosin, A. Albinati, Organometallics 18 (1999) 4591.

[2] (a) R.F. Heck, Acc. Chem. Res. 12 (1979) 146. (b) R.F. Heck, Comprehensive Organic Synthesis, vol. 4, Pergamon, Oxford, (1991). (c) M.J. Brown, K.K. Hii, Angew. Chem. 108 (1996) 679. (d) M.J. Brown, Chem. Soc. Rev. (1993) 25. (e) M. Tschoerner, P.S. Pregosin, A. Albinati, Organometallics 18 (1999) 670. (f) A. de Meijere, F.E. Meyer, Angew.Chem. 106 (1994) 2473.

[3] (a) A. Pfaltz, Acta Chim. Scand. 50 (1996) 189. (b) O. Reiser, Angew. Chem. 105 (1993) 576. (c) B.M. Trost, D.L. van Vranken, Chem. Rev 96 (1996) 395.

[4] (a) L. Canovese, F. Visentin, P. Uguagliati, G. Chessa, A. Pesce, J. Organomet. Chem. 566 (1998) 61. (b) B. Crociani, S. Antonaroli, G. Bandoli, L. Canovese, F. Visentin, P. Uguagliati, Organometallics 18 (1999) 1137. (c) K. Selvakumar, M. Valentini, M. Wörle, P.S. Pregosin, A. Albinati, Organometallics 18 (1999)1207.

[5] (a) B. Crociani, F. Di Bianca, P. Uguagliati. L. Canovese, A. Berton, J. Chem. Soc. Dalton Trans. (1991) 71. (b) B. Crociani, S. Antonaroli, F. Di Bianca, L. Canovese, F. Visentin, P. Uguagliati, J. Chem. Soc. Dalton Trans. (1994) 1145. (c) L. Canovese, F. Visentin, P. Uguagliati, F. Di Bianca, S. Antonaroli, B. Crociani, J. Chem. Soc. Dalton Trans. (1994) 3113. (d) L. Canovese, F. Visentin, P. Uguagliati, B. Crociani, F. Di Bianca, Inorg. Chim. Acta 235 (1995) 45. (e) B. Crociani, S. Antonaroli, M. Paci, F. Di Bianca, L. Canovese, Organometallics 16 (1997) 384. (f) L. Canovese, F. Visentin, P. Uguagliati, G. Chessa, V. Lucchini, G. Bandoli, Inorg. Chim. Acta 275 (1998) 385. (g) L. Canovese, F. Visentin, G. Chessa, A. Niero, P. Uguagliati, Inorg. Chim. Acta 293 (1999) 44. (h) B. Crociani, S. Antonaroli, L. Canovese, F. Visentin, P. Uguagliati, Inorg. Chim. Acta submitted.

[6] (a) L. Canovese, F. Visentin, P. Uguagliati, B. Crociani, J. Chem. Soc. Dalton Trans. (1996) 1921. (b) L. Canovese, F. Visentin, G. Chessa, P. Uguagliati, A. Dolmella, J. Organomet. Chem. 601 (2000) 1.

[7] (a) R. Van Asselt, C.J. Elsevier, W.J.J. Smeets, A.L. Speck, Inorg. Chem. 33 (1994) 1521. (b) P.T. Cheng, C.D. Cook, S.C. Nyburg, K.Y. Wan, Inorg. Chem. 10 (1971) 2210. (c) F. Ozawa, T. Ito, Y. Nakamura, A. Yamamoto, J. Organomet. Chem. 168 (1979) 375. (d) R. Van Asselt, C.J. Elsevier, Tetrahedron 50 (1994) 323. (e) F. Gomez-de la Torre, F.A. Jalon, A. Lopez-Agenjo, B.R. Manzano, A. Rodriguez, T. Sturm, W. Weissensteiner, M. Martinez-Ripoll, Organometallics 17 (1998) 4634 and references therein. (f) M. Tschoerner, G. Trabesinger, A. Albinati, P.S. Pregosin, Organometallics 16 (1997) 3447.

[8] (a) P. Wehman, R.E. Rülke, V.E. Kaasjager, P.C.J. Kamer, H. Kooijman, A.L. Spek, C.J. Elsevier, K. Vrieze, P.W.N.M. van Leeuwen, J. Chem. Soc. Chem. Commun. (1995) 331. (b) R.E. Rülke, V.E. Kaasjager, P. Wehman, C.J. Elsevier, P.W.N.M. van Leeuwen, K. Vrieze, J. Fraanje, K. Goubitz, A.L. Spek, Organometallics 15 (1996) 3022.

[9] H.D. Beckhaus, Angew. Chem. 17 (1978) 593.

[10] P. Uguagliati, A. Benedetti, S. Enzo, L. Schiffini, Comput. Chem. 8 (1984) 161.

[11] L. Canovese et al. preliminary results.

[12] L. Canovese, G. Chessa, G. Marangoni, B. Pitteri, P. Uguagliati, F. Visentin, Inorg. Chim. Acta 186 (1991) 79.

[13] T. Ukai, H. Kawazura, Y. Ishii, J.J. Bonnet, J.A. Ibers, I. Organomet. Chem. 65 (1974) 253.

[14] (a) M. Baboulène, J.L. Torregrosa, V. Spéziale, A. Lattes, Bull. Soc. Chim. Fr. II (1980) 565. (b) N. Tokitoh, R. Okazaki, Bull. Chem. Soc. Jpn. 61 (1988) 735.

[15] G. Balacco, J. Chem. Inf. Comput. Sci. 34 (1994) 1235.

[16] D.W. Marquardt, SIAM J. Appl. Math. 11 (1963) 431.